Energy Spectra of Cosmic Rays Accelerated at Ultrarelativistic Shock Waves

J. Bednarz and M. Ostrowski

Obserwatorium Astronomiczne, Uniwersytet Jagielloński, ul Orla 171, 30-244 Kraków, Poland

(Received 31 October 1997)

Energy spectra of particles accelerated by the first-order Fermi mechanism are investigated at ultrarelativistic shock waves, outside the range of Lorentz factors considered previously. For particle transport near the shock a numerical method involving small amplitude pitch-angle scattering is applied for flows with Lorentz factors γ from 3 to 243. For large γ shocks a convergence of derived energy spectral indices up to the value $\sigma_\infty \approx 2.2$ is observed for all considered turbulence amplitudes and magnetic field configurations. Recently the same index was derived for γ-ray bursts by Waxman [Astrophys. J. Lett. **485**, L5 (1997)]. [S0031-9007(98)05784-6]

PACS numbers: 98.70.Sa, 98.70.Rz

In currently favored gamma-ray burst (GRB) models optically thin emitting regions move relativistically, with Lorentz factors of order of a few hundreds (cf. a review [1]). The power-law form of the spectrum often observed at high photon energies suggests the existence of nonthermal population of energetic particles. It was also proposed that GRB sources may produce cosmic ray particles with extremely high energies [2]. Thus modeling of burst sources requires a discussion of particle acceleration processes, possibly Fermi acceleration at ultrarelativistic shock waves.

The work of Kirk and Schneider [3] opened the problem of cosmic ray acceleration at relativistic shock waves for quantitative consideration. Substantial progress since that time (e.g., Heavens and Drury [4], Kirk and Heavens [5], Begelman and Kirk [6], Ostrowski [7], Bednarz and Ostrowski [8]; for a review, see Ostrowski [9] and Kirk [10]) clarified a number of issues related to shock waves with velocities reaching $0.98c$ or the Lorentz factor $\gamma \simeq 5$, but —to our knowledge— no one has attempted to discuss particle acceleration at shocks moving with ultrarelativistic velocities characterized with large factors $\gamma \gg 1$.

The main difficulty in modeling an acceleration process at shocks with large γ is the fact that involved particle distributions are extremely anisotropic in shock, with the particle angular distribution opening angles $\sim\gamma^{-1}$ in the upstream plasma rest frame. When transmitted downstream the shock particles have a limited chance to be scattered so efficiently to reach the shock again, but the energy gain of any such "successful" particle can be comparable to its original energy. As pointed out by Bednarz and Ostrowski [8] any realistic model of particle scattering at magnetohydrodynamic turbulence close to the relativistic shock cannot involve large-angle pointlike scattering. The choice is either to integrate exactly particle equations of motion in some "realistic" structure of the perturbed magnetic field, or to use a small-angle scattering model for particle momentum. With the angular scattering amplitude $\Delta\Omega \ll \gamma^{-1}$ and the mean scattering time Δt not too short [$\Delta t \geq T_g(\Delta\Omega)^2$, where T_g is the particle gyration period], the last model reproduces the pitch-angle diffusion process at small amplitude waves. We prefer that approach to the exact integration of equations of motion of a particle because of its relative simplicity. It is also suggested that it can be reasonably used for modeling particle trajectories in turbulent fields with large amplitude, if small Δt [$\leq T_g(\Delta\Omega)^2$] is involved. Below, a hybrid method involving the small amplitude pitch-angle scattering is applied for a particle transport near the shock for flows with Lorentz factors γ from 3 to 243.

I. Numerical simulations.—In the present considerations we model a process of cosmic ray particle acceleration by applying the following Monte Carlo approach (cf., e.g., [8]). Energetic seed particles are injected at the shock and each particle trajectory is followed using numerical computations until it escapes through the free escape boundary placed far downstream from the shock or it reaches the energy larger than the upper energy limit at $E_{\max} = 10^{10}E_0$ (E_0—initial energy). Simulations are continued until one obtains the power-law spectrum in the full range $(E_0, E_{\max})$ (cf. [7,8]). All computations are performed in the respective—upstream or downstream—plasma rest frame. Each time when the particle crosses the shock its momentum is Lorentz transformed to the respective plasma rest frame and, in the shock normal rest frame (cf. [6]; henceforth "shock rest frame") the respective contribution is added to the given momentum bin in the particle spectrum. In the simulations we use a simple trajectory splitting technique. All particles are injected into simulations with the same initial weight factors 1.0. When some particles escape through the boundary, we replace them with ones arising from splitting the remaining high-weight particles in a way to preserve its phase space coordinates, but ascribing only a half or a smaller respective part of the original particle weight to each of the resulting particles. For any particle crossing the shock a factor is added to the simulated spectrum in the shock rest frame equal to the particle weight divided by its velocity component normal to the shock.

Efficient particle scattering with a very small $\Delta\Omega$ requires derivation of a large number of scattering acts and

the respective numerical code becomes extremely time-consuming. In order to overcome this difficulty in the present simulations we propose a hybrid approach involving very small $\Delta\Omega_1$ ($\ll\gamma^{-1}$) close to the shock, where the scattering details play a role, and much larger scattering amplitude $\Delta\Omega_2 = 9°$ to describe particle diffusion further away from the shock. The respective scaling of the scattering time Δt is performed in both cases ($\Delta\Omega_1^2/\Delta t_1 = \Delta\Omega_2^2/\Delta t_2$) to mimic the same turbulence amplitudes measured by the values of the cross-field diffusion coefficient, $\kappa_\perp$, and the parallel diffusion coefficient, $\kappa_\parallel$.

For a few instances we checked the validity of this approach by reproducing the results for the small $\Delta\Omega_1$ everywhere. In the present simulations we assume the same scattering conditions upstream and downstream from the shock (the same $\kappa_\perp$ and $\kappa_\parallel$ in the units of $r_g c$, where $r_g c$ is the particle gyration radius in the unperturbed background magnetic field), preserving particle energy at each scattering in the plasma rest frame. In the simulations we considered a few configurations of the upstream magnetic field, with inclinations with respect to the shock normal being $\psi = 0°$, $10°$, $20°$, $30°$, $60°$, and $90°$. The first case represents the parallel shock, the second is for the oblique shock—subluminal (i.e., with the shock velocity projection at the magnetic field with slower than light velocity) at $\gamma = 3$ and a superluminal one at larger γ, and the larger ψ are for superluminal perpendicular shocks for all velocities. The downstream magnetic field is derived for the relativistic shock with the compression R obtained with the formulas of Heavens and Drury [4] for a cold (e, p) plasma—$R \approx 3.6$ for our smallest value of $\gamma = 3$ and tends to $R = 3$ for $\gamma \gg 1$, as measured in the shock rest frame.

II. Results.—Particle spectral indices were derived for different mean magnetic field configurations, measured by the magnetic field inclination ψ with respect to the shock normal in the upstream plasma rest frame, and for different amounts of turbulence measured by $\kappa_\perp/\kappa_\parallel$.

In successive panels in Fig. 1 the energy spectral indices, σ, for varying ψ and $\kappa_\perp/\kappa_\parallel$ are presented. For a parallel shock ($\psi = 0°$) the amount of scattering does not influence the spectral index and for growing γ it approaches $\sigma_\infty \simeq 2.2$. One may note that essentially the same limiting value was anticipated for the large-γ parallel shocks by Heavens and Drury [4]. The results for $\psi = 10°$ are for superluminal shocks if $\gamma > 5.75$.

In this case, when we go from the "slow" $\gamma = 3$ shocks to higher γ ones, at first the spectrum inclination increases (σ grows), but at large γ the spectrum flattens to approach the asymptotic value close to 2.2. The spectrum steepening phase is more pronounced for small amplitude perturbations (small $\kappa_\perp/\kappa_\parallel$), but even at very low turbulence levels the final range of the spectrum flattening is observed. For larger ψ the situation does not change considerably, but the phase of spectrum steepening is wider, involving larger values of σ and starting at smaller velocities, below the lower limit of our considerations (there may be no such range involving the small steepening phase if the required velocity is below the sound velocity). The spectral indices for different magnetic field inclinations, but for the same value of $\log_{10}(\kappa_\perp/\kappa_\parallel) = -3.44$, are presented in Fig. 2.

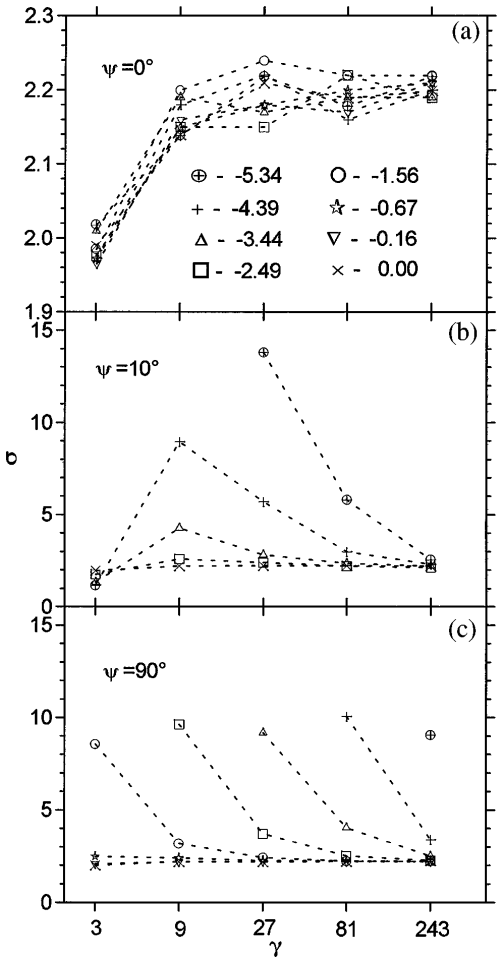

FIG. 1. The simulated spectral indices σ for particles accelerated at shocks with different Lorentz factors γ. Results for a given $\kappa_\perp/\kappa_\parallel$ are joined with lines; the respective value of $\log_{10}\kappa_\perp/\kappa_\parallel$ is marked by the point shape (see upper panel). The results for different magnetic field inclinations ψ are given in the successive panels: (a) $\psi = 0°$, (b) $\psi = 10°$, and (c) $\psi = 90°$.

The large spectral indices occurring in the steepening phase are usually interpreted as a spectrum cutoff. In this case the main factor increasing the particle energy density is a nonadiabatic compression in the shock [6]. The particle angular distributions $F(\mu)$ in the considered shocks can be extremely anisotropic when considered in the upstream plasma rest frame. However, when presented in the shock rest frame the distribution is always "mildly" anisotropic. This feature is illustrated in Fig. 3 for γ equals 3 or 27 (note that in Figs. 3–6 the area below each curve is normalized to 100). In simulations we observed an interesting phenomenon accompanying previously discussed spectrum convergence to the limiting inclination: spectra close to the limit exhibit similar angular dis-

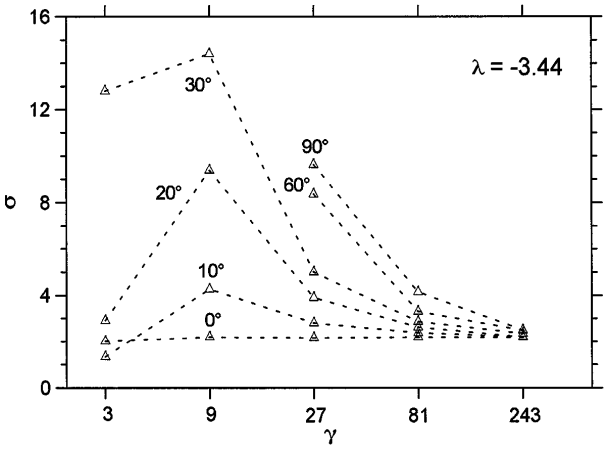

FIG. 2. The simulated spectral indices σ for particles accelerated at shocks with different Lorentz factors γ. Results for a given upstream magnetic field inclination ψ are joined with dashed lines; the respective value of ψ is given near each curve. The value $\lambda \equiv \log_{10}(\kappa_\perp/\kappa_\parallel)$ is given in the figure.

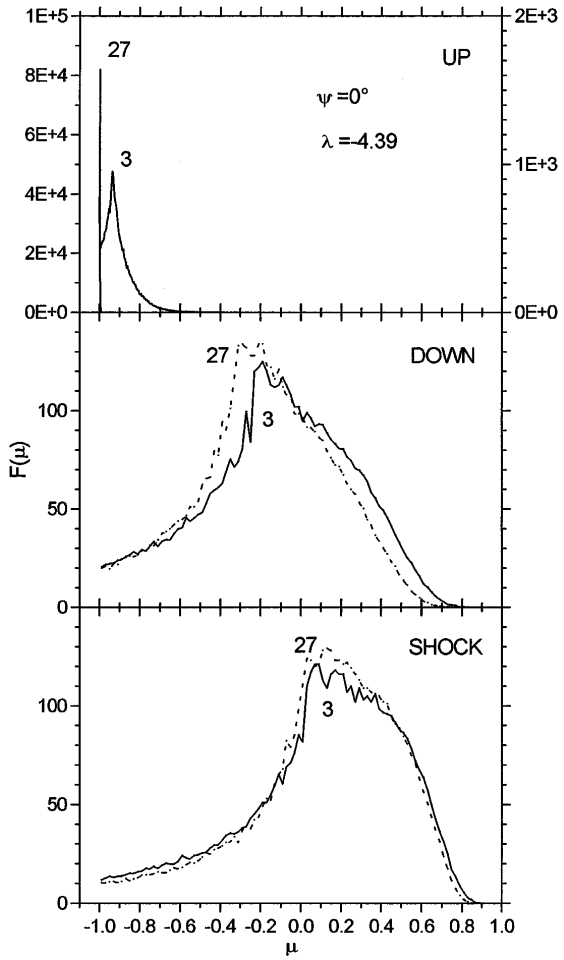

FIG. 3. The simulated particle angular distributions in the shock in different coordinate frames: UP: the upstream plasma rest frame, DOWN: the downstream plasma rest frame, and SHOCK: the shock rest frame. The results are presented for parallel shocks with the Lorentz factors 27 and 3 given near the respective curves. In the upper panel the left axis is for $\gamma = 27$ and the right one for $\gamma = 3$.

tributions at the shock *as measured in the shock rest frame* (Fig. 4). Again, this feature is independent of the background conditions, and the difference between the actual angular distribution and the limiting one reflects the difference between the spectral index σ and σ_∞ (cf. Fig. 5). For parallel shocks with $\gamma \geq 9$, where the spectral index is essentially constant $\sigma = \sigma_\infty$, this distribution is independent of the value of γ and the perturbation amplitude $\kappa_\perp/\kappa_\parallel$ (Fig. 6).

III. Discussion.—For large γ shocks we observe the convergence of the derived energy spectral indices to the value $\sigma_\infty \approx 2.2$, independently of background conditions. This unexpected result providing a strong constraint for the acceleration process in large γ shocks requires a more detailed analysis. Particularly, the acceleration process in the superluminal shocks has to be clarified in the presence of the small amplitude turbulence.

The inspection of particle trajectories reveals a simple picture of acceleration. Cosmic ray particles are wandering in the downstream region with the shock wave moving away with the mildly relativistic velocity $\approx c/3$. Some of these particles succeed to reach the shock, but then they remain in the upstream region for a very short time—being very close to the shock—due to large shock velocity $\approx c$. This scenario is essentially equivalent to the picture involving particles reflecting in a nonelastic way from the receding wall.

For large γ shocks any particle crossing the shock upstream has a momentum vector nearly parallel to the shock normal (cf. Ostrowski [7]); e.g., for $\gamma = 243$ the momentum inclination must be smaller than $\theta_{\max} \approx 0.24°$. If the scattering or the movement along the curved trajectory increases this inclination above the mentioned limiting value the particle tends to recross the shock downstream. One should note that even a tiny—comparable to $\theta_{\max}$—angular deviation in the upstream plasma ($\Delta\theta_U$) can lead to large angular deviation for $\gamma \gg 1$ as observed in the downstream rest frame.

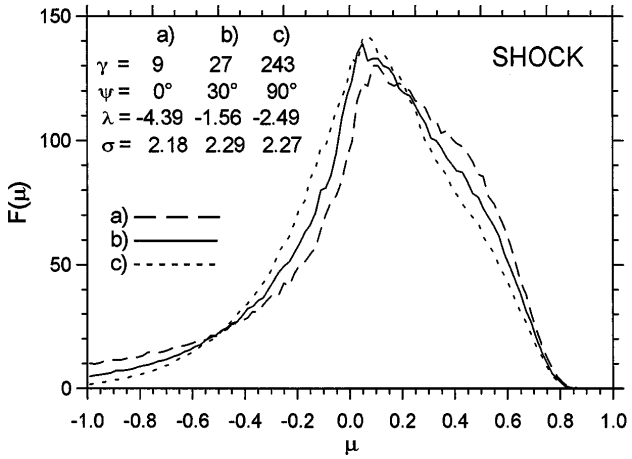

FIG. 4. Examples of the shock rest frame particle angular distributions for different cases with σ close to σ_∞.

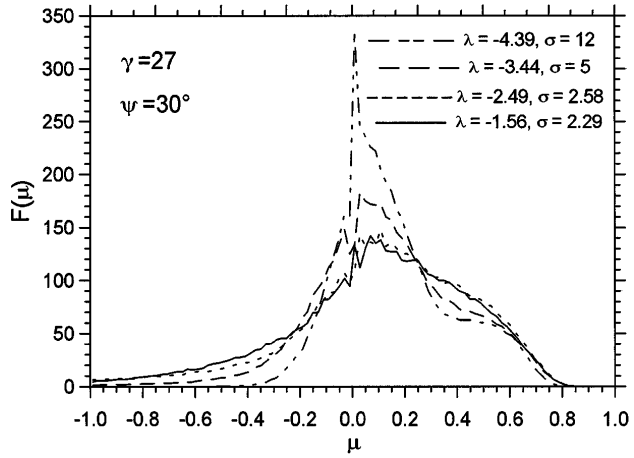

FIG. 5. The shock rest frame particle angular distributions for $\gamma = 27$ and $\psi = 30°$. Curves are presented for increasing $\lambda \equiv \log_{10} \kappa_\perp/\kappa_\parallel$ and σ approaching σ_∞. The last curve is the same as curve (b) in Fig. 4.

The phenomenon of decreasing σ to σ_∞ at constant λ and for growing γ results from *slower diminishing of the part of* $\Delta\theta_U$ *caused by scattering in comparison to* $\Delta\theta_U$ *arising due to trajectory curvature* in the uniform field component. In this way the magnetic field structure defined by ψ becomes unimportant, at least for $\gamma \to \infty$ (one should also note that the downstream field inclination approaches 90° if $\psi \neq 0$ and $\gamma \gg 1$). As a result particles crossing the shock downstream are scattered in a wide angular range with respect to the shock normal, providing some particles with the trajectory phase parameter allowing for recrossing the shock upstream even for the perpendicular magnetic field configuration. Our interesting finding, not fully explained with such simple arguments, is of the belief that the resulting spectral index is the same for oblique and parallel shocks.

We also observe that when approaching the limiting value of the spectral index the mean particle energy gain $\langle \Delta E/E \rangle$ in the cycle "upstream-downstream-upstream" reaches a value close (slightly above) to 1.0, much smaller than a factor γ^2 expected for a model involving a large angle pointlike scattering. Thus the particle acceleration time scale, as measured in the downstream plasma rest frame, can be roughly estimated as a fraction of the gyration time in this region.

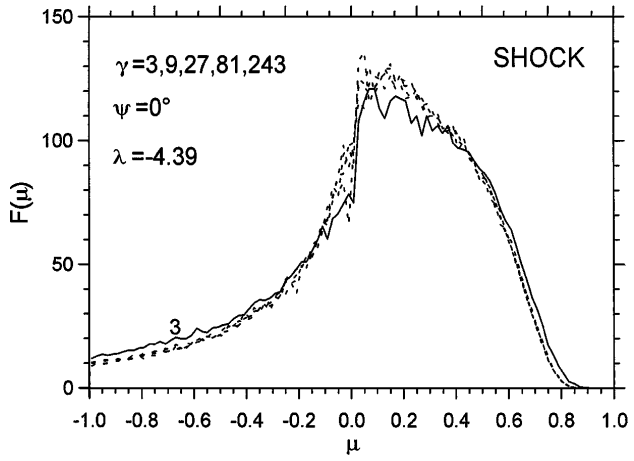

FIG. 6. The shock rest frame particle angular distributions for parallel shocks with $\gamma = 3$, 9, 27, 81, and 243. A visible deviation of the distribution for $\gamma = 3$ (full line) results from the slightly larger compression occurring in such a shock.

IV. Final remarks.—The presented results are to be applied in models of GRB sources involving ultrarelativistic shock waves. One should note that the mean downstream plasma proton energies can reach there several tens of GeV (cf. Paczyński and Xu [11]) and the lower limit of the considered cosmic ray energies has to be larger than this scale. For shocks propagating in (e^-, e^+) plasma the involved thermal energies are lower, $\sim\gamma$ MeV. These estimates provide the respective lower limits for the accelerated cosmic ray particles. For the physical conditions considered in GRB sources the acceleration process can provide particles with much larger energies, limited only by the condition that the energy loss processes (radiative, or due to escape) are ineffective in the downstream gyroperiod time scale. We note a striking coincidence of our limiting spectral index with the value 2.3 ± 0.1 derived for energetic electrons from gamma-burst afterglow observations [12].

Our derivations are limited to the test particle approach. However, as the obtained spectra are characterized with $\sigma > 2.0$, any nonlinear back reaction effects are not expected to affect the acceleration process within the spectrum high energy tail with $\sigma \approx \sigma_\infty$.

The present work was supported by the *Komitet Badań Naukowych* through Grant No. PB 179/P03/96/11.

[1] T. Piran, astro-ph/9801001, in Proceedings of the Fifth Conference on Underground Physics 1997 (TAUP97) (to be published).
[2] E. Waxman, Phys. Rev. Lett. **75**, 386 (1995).
[3] J. G. Kirk and P. Schneider, Astrophys. J. **315**, 425 (1987).
[4] A. Heavens and L'O. C. Drury, Mon. Not. R. Astron. Soc. **235**, 997 (1988).
[5] J. G. Kirk and A. Heavens, Mon. Not. R. Astron. Soc. **239**, 995 (1989).
[6] M. C. Begelman and J. G. Kirk, Astrophys. J. **353**, 66 (1990).
[7] M. Ostrowski, Mon. Not. R. Astron. Soc. **249**, 551 (1991).
[8] J. Bednarz and M. Ostrowski, Mon. Not. R. Astron. Soc. **283**, 447 (1996).
[9] M. Ostrowski, in *Proceedings of the International Symposium on Extremely High Energy Cosmic Rays, Tanashi, 1996*, edited by M. Nagano (ICRR, Tanashi, 1996), p. 68.
[10] J. G. Kirk, in *Proceedings of the International Conference on Relativistic Jets in AGNs, Cracow, 1997*, edited by M. Ostrowski *et al.* (OAUJ, Cracow, 1997), p. 145.
[11] B. Paczyński and G. Xu, Astrophys. J. **427**, 708 (1994).
[12] E. Waxman, Astrophys. J. Lett. **485**, L5 (1997).